Final Report:

MIE 697CE - Ocean Renewable Energy
Semester Project

Design of a Monopile Support Structure for the IEA 15 MW Reference Turbine

---

Author:
Jacob Davis

May 5, 2020

Content

Executive Summary

This document presents a discussion of the structural design and analysis of a monopile support structure for the International Energy Agency 15 MW reference offshore wind turbine. Structural design procedures are carried our in adherence to the International Electrotechnical Commission (IEC) standards 61400-1 and 61400-3-1 pertaining to the general design of wind turbines and design of fixed offshore wind turbines, respectively. Estimates of aerodynamic, hydrodynamic, and other external loading conditions are calculated based on the site-specific metocean conditions provided by the developer and are presented in detail. The development of a coupled structural finite element analysis model of the turbine tower and monopile structure is described, along with the use of the model to perform a parametric optimization on the dimensions of the monopile substructure. In conclusion of the study, a final design recommendation is presented.

General Information

Choice of Codes and Standards: The design and validation of the monopile substructure will be performed in accordance to the IEC 61400-1 and 61400-3-1 standards. In particular, specific reference will be made to section 7, **Structural Design**, of both 61400-1 and 61400-3-1 [1, 2]. Relevant subsections include General (7.1), Design methodology (7.2), Loads (7.3), Load and load effect calculations (7.5), and Ultimate limit state analysis (7.6). Subsection 7.4, Design situations and load cases, will be excluded on the basis that the developer has provided the following operating and survival design conditions: 1) turbine operating at rated wind speed in a one-year storm; and 2) turbine stopped in a 50-year maximum wind speed condition, considering both flapwise and feathered blade pitch orientations. All environmental loads will be calculated based on site-specific metocean conditions provided by the developer in **table 1**. Furthermore, the developer has provided an additional subset of design performance requirements, shown in **table 2**. Details of the IEA 15 MW turbine and blades are provided in **tables 10 and 11** of the appendix.

Table 1: Metocean Conditions [3].

Parameter	50 Year Return	1 Year Return
Significant wave height	9.0 m	6.0 m
Maximum wave height	16.86 m	11.1 m
Peak period	13.56 s	8.0 s
Wave spectrum	PM	PM
Max. wind speed (10 min mean at 120 m)	40 m/s	U_{rated}
Wind gust spectrum	Von Karman	Steady

Table 2: Developer Performance Requirements [3].

Requirement	Specification
Bending mode natural frequency	$1P < f_n < 3P$ (soft-stiff) $f_n \notin f_{wave}, f_{wind}$
Tower top displacement	Less than 1% of total structure height at U_{rated}

General Assumptions

The following loads will be considered per section 7.3, Loads: 1) Gravitational and inertial (7.3.2); 2) Aerodynamic (7.3.3); 3) Actuation (7.3.4); and 4) Hydrodynamic (7.3.5). At present, Sea/lake ice loads (7.3.6) and Other loads (7.3.7) will be excluded in the focus of this project on the basis that the necessary information required to estimate such loading has not been provided by the developer.

Starting Design

The starting design is a monopile designed for the IEA 10 MW reference turbine which has a uniform outer diameter of 9.0 m, top inner diameter of 8.7 m, and base inner diameter of 8.8 m (**Appendix, table 13**) [4]. Design iterations will begin with analytical estimates of the stresses, deflection, natural frequency, and critical buckling load, before progressing to a full structural analysis in the finite element analysis software, ANSYS. A nonlinear continuum model will be used to model the effects of soil stiffness.

Aerodynamic Load Calculations

Turbine Forces: The thrust force design condition 1 (operating condition) was obtained using the power and thrust curve provided in the IEA 15 MW definition document and shown in **figure 1** [5]. This yields an approximate **operating thrust of 2.75 MN** at the rated speed of 10.59 m/s. To estimate the thrust forces for design condition 2 (stopped), the blade was discretized into segments and incremental lift and drag forces were computed along the blade length for angles of attack corresponding to the feathered ($\theta_{p,0} = 90$ deg) and flapwise ($\theta_{p,0} = 0$ deg) blade pitches (relative to the tip). This procedure was carried out in a self-written MATLAB script, *stopped rotor blade loads.m*. The script utilizes AeroDyn *.dat* blade files and associated airfoil files to obtain the corresponding airfoil ID, and thus polars, as well as the local chord, thickness, and twist for each section along the blade. To run properly for this scenario, "*IEA-15-240-RWT AeroDyn15 blade.dat*" and "*IEA-15-240-RWT AeroDyn15 Polar xx.dat*" files are required [5]. Their corresponding directories must also be input into the script. The results of this analysis, provided in **Appendix, tables 14 and 15**, yields a thrust force of **0.09 MN for the feathered condition** and **1.75 MN for the flapwise condition**. For the feathered condition, an additional **bending moment at the monopile base (seabed) of 12.8 MN-m** was calculated from lift forces acting tangential to the rotor plane. This bending moment was negligible for the flapwise condition. Thrust and tangential forces for both load conditions are shown as a function of blade position in **figure 2**.

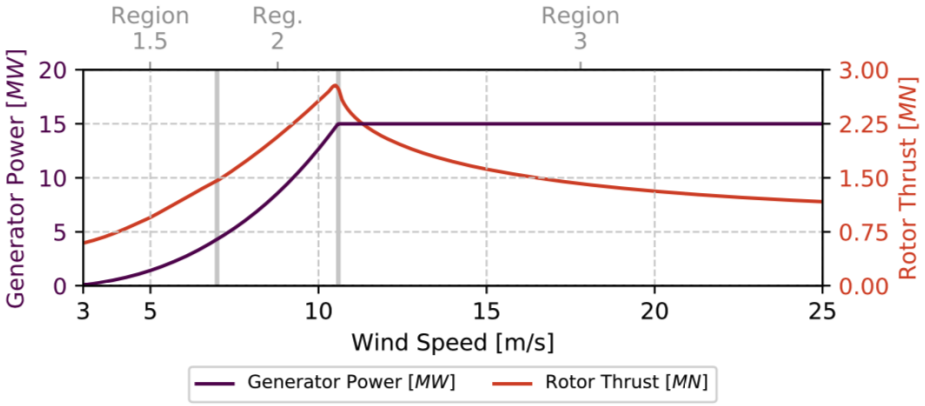

Figure 1: IEA 15 MW Offshore Wind Turbine Power and Thrust Curves [5].

Tower Drag: Similar to the calculation of blade thrust forces, tower drag loads were obtained by discretizing the tower into a finite number of sections and computing the drag forces along the height. This procedure is carried out in the self-written *tower drag.m* script. The script allows for the input of a tower data file and a drag coefficient data file. Both files are read, and the drag coefficient data file is re-sampled to enable the reliable look-up of drag coefficients. The script loops through the tower sections, and for each iteration, it obtains the tower or exposed monopile diameter, calculates the Reynolds number based on diameter, matches the Reynolds number with the drag coefficient data file, and computes the drag force on the section. The results are prepared in an output file for later coupling with ANSYS Workbench. The files used in this analysis include the "*IEA 15MW Tower and 10MW Monopile Data to Waterline.csv*" tower file, and drag coefficient data for a smooth cylinder "*smooth cylinder.csv*" provided in Munson et al. *Fundamentals of Fluid Mechanics, 6e* and appended in **Appendix, figure 18**.

To account for variations in the vertical wind speed boundary layer, a wind shear log law profile was assumed:

$$\frac{U(z)}{U(z_r)} = \frac{ln(z/z_0)}{ln(z_r/z_0)}$$

Where U represents the wind speed, z and z_r represent the height and reference height, respectively, and z_0 represents the surface roughness. A value for offshore surface roughness was calculated based on the following fit proposed by Taylor and Yelland (2001):

$$\frac{z_0}{H_s} = 1200 \left(\frac{H_s}{L_p}\right)^{4.5}$$

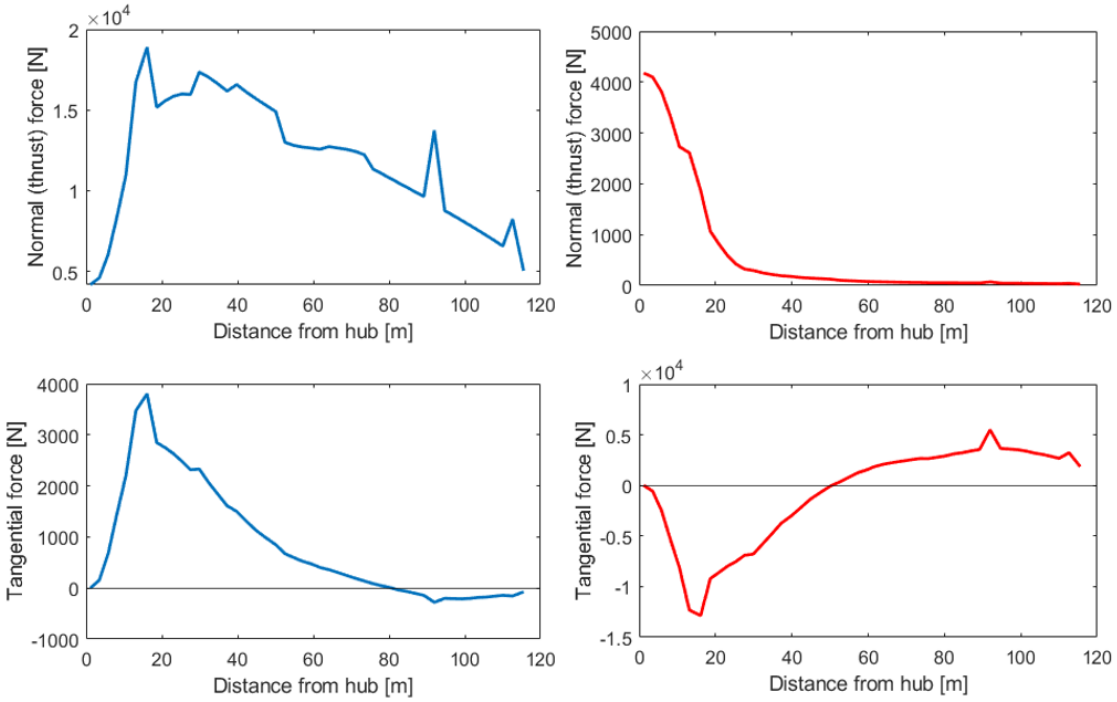

Figure 2: 50-yr return wind turbine forces as a function of blade position for flapwise (left, blue) and feathered (right, red). Forces in the directions normal and tangential to the rotor plane are shown.

Where H_s and L_p are the significant wave height and peak wavelength obtained from the developer's site assessment. The results of this analysis yield the drag force profiles shown in **figure 3**. The total drag force on the tower is **54 kN** for the 1-year wind speed and **688 kN** for the 50-year wind speed. Despite the increasing wind speed at high heights, the decrease in drag beyond 50 m is due to the tapering of the tower diameter. These forces will later be applied to the finite element model.

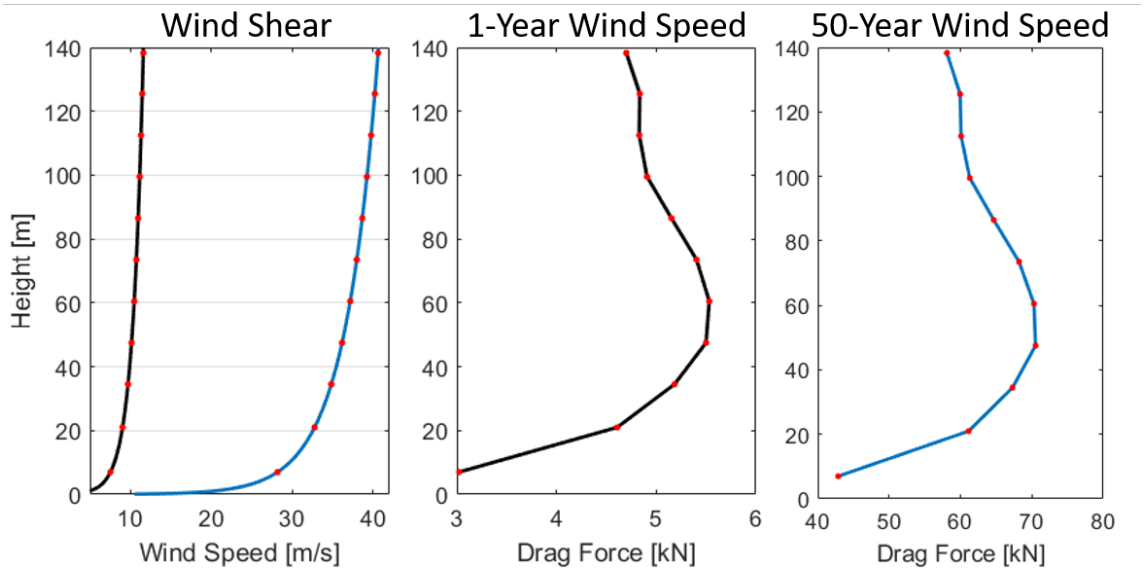

Figure 3: Wind shear (left) and tower drag force profiles for 1-year wind speed of 10.59 m/s (black, middle) and 50-year wind speed of 40 m/s (blue, right). The red dots indicate midsection nodes.

Hydrodynamic Load Calculations

Analytical Wave Force and Moment Values: An initial estimate of the wave loads was obtained by applying a Morison equation discretization approach to the starting design, the IEA 10 MW monopile [4]. As a first approach, this method is deemed valid as the ratios of monopile diameter to wavelength, $9/96 = 0.094$ for the 1-year return sea state and $9/207 = 0.043$ for the 50-year return sea state, are less than the commonly accepted limit of 0.2 [6]. The force and moment values for the 1-year return wave were obtained as **6.71 MN** and **123.98 MN-m**, respectively. Similarly, for the 50-year return wave, values were obtained as **6.91 MN** and **110.33 MN-m** (**figure 4**). The"*monopile morison.m*" script used to perform this calculation. Much like the tower drag script, the Morison wave load script requires input of added mass and drag coefficient data. The data used for this project, "*CM vs KC cylinder.csv*" and "*wave amp vs KCdivCDS.csv*," were obtained from DNV-OS-J101 [7]. Drag and added mass coefficient operating points for both load conditions are shown in **Appendix, figure 19**. The script was successfully validated against similar Morison results for both Leite and Pereyra et al. [6, 8].

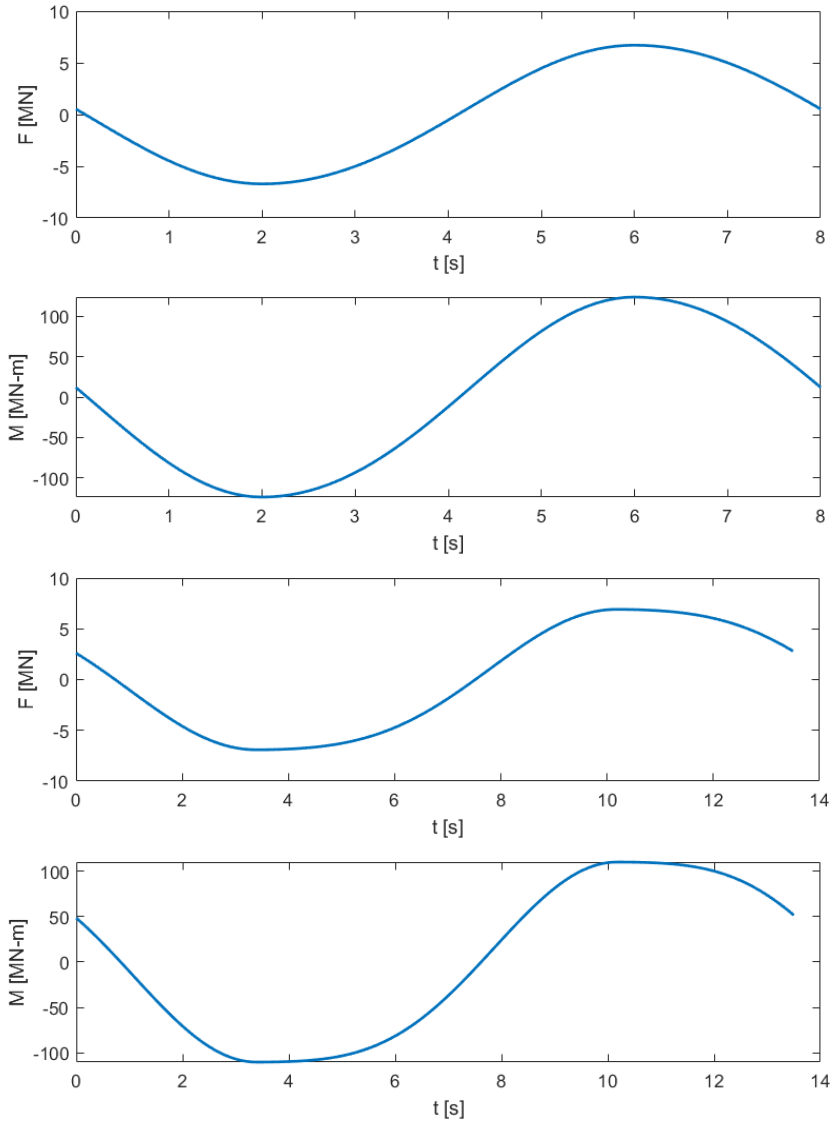

Figure 4: Morison-calculated wave loads as a function of wave period for 1-year return (top two images) and 50-year return (bottom two images) wave. The monopile is assumed rough ($C_{DS} = 1.05$) for the first 20 m of depth (due to marine biofouling) and smooth ($C_{DS} = 0.65$) below 20 m.

Computational Wave Pressures: To obtain a more accurate hydrodynamic pressure distribution on the monopile, as well as to incorporate a method for determining wave loads which can be parameterized and directly coupled to the finite element model, the boundary element method solver ANSYS Aqwa was used. Aqwa allows for the calculation of incident, diffracted, and radiated velocity potentials. As the monopile is assumed to be rigid in this analysis, radiated potentials are not calculated.

Setup: Only 30 meters (equal to the water depth) of the monopile are included in the analysis. The upper 27.5 m of the monopile was meshed with diffracting elements while the lower 2.5 m (closest the seabed) was defined as non-diffracting (since Aqwa returns errors if diffracting elements are placed to close to the seabed). In total, 672 diffracting panel elements with an average size of 1 m were used. Simulations were run for four wave directions (0,90,180, and 270 degrees) with frequencies from 0.07375 Hz (13.46 s) to 0.125 Hz (8 s). Depictions of the wave surface elevation are shown in **figure 6**.

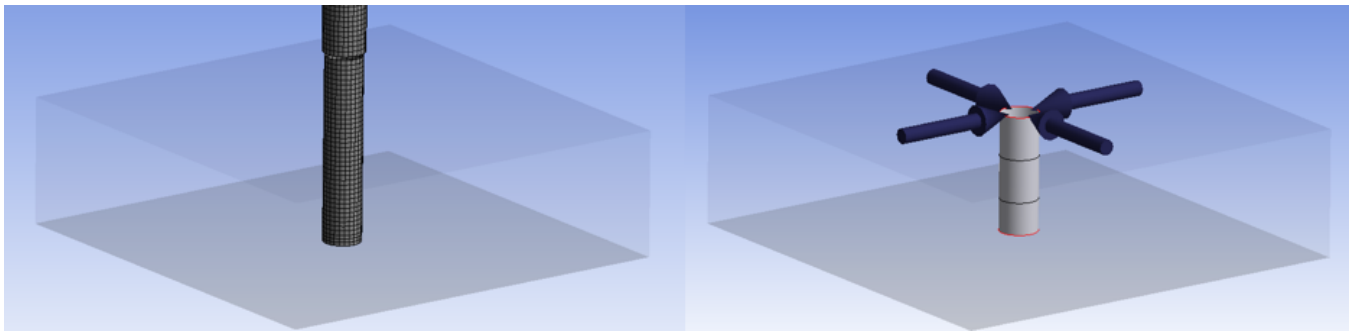

Figure 5: ANSYS Aqwa computational domain setup. The meshed monopile (left) and wave setup (right) are shown.

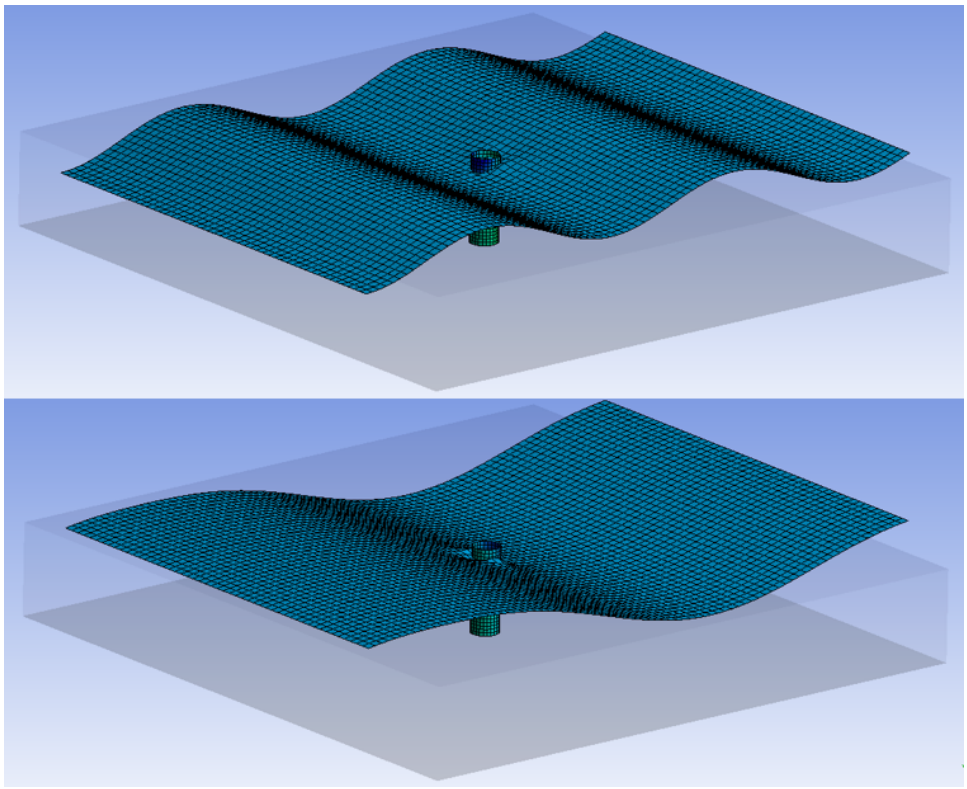

Figure 6: ANSYS Aqwa wave surface elevation simulation. 1-year wave with an amplitude of 5.55 m and 8.0 s period (top) and 50-year wave with an amplitude of 8.43 m and 13.56 s period (bottom).

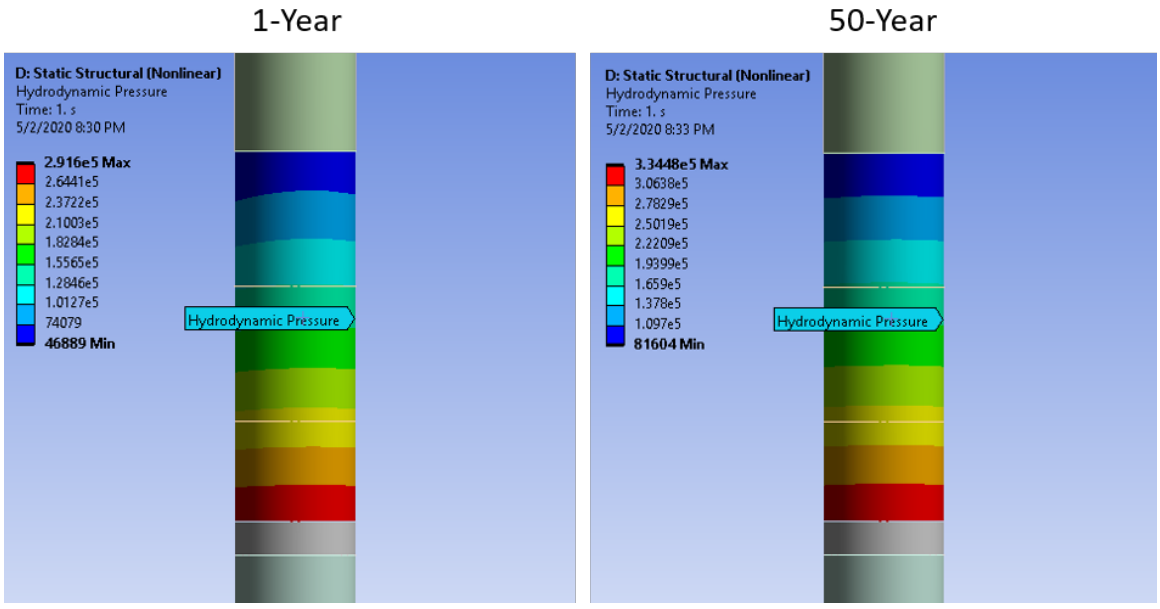

Figure 7: ANSYS Aqwa monopile surface hydrodynamic pressures. 1-year wave with an amplitude of 5.55 m and 8.0 s period (left) and 50-year wave with an amplitude of 8.43 m and 13.56 s period (right).

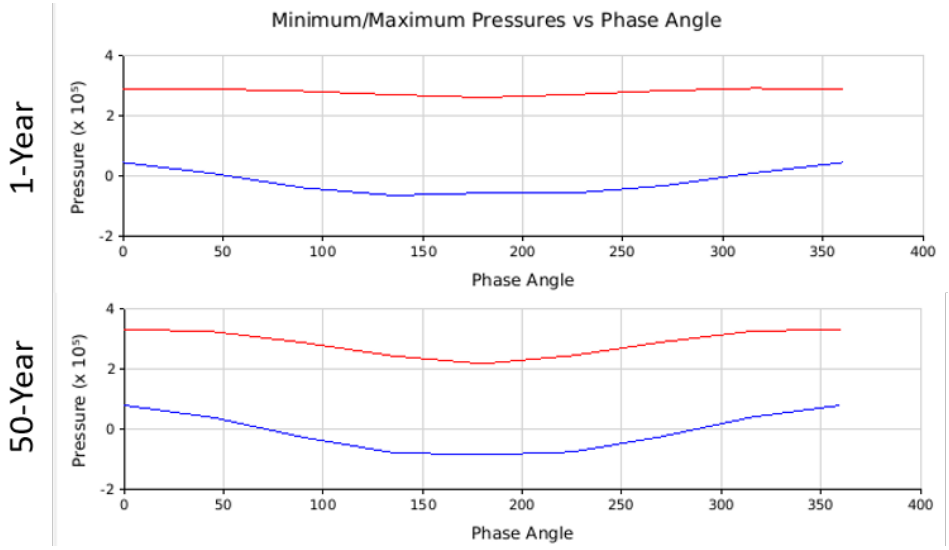

Figure 8: ANSYS Aqwa hydrodynamic pressures as a function of phase.

Results: Hydrodynamic pressure distributions computed in ANSYS Aqwa are shown in **figure 7**. The maximum pressure at any section is **0.292 MPa** for 1-year wave and **0.335 MPa** for the 50-year wave. Maximum and minimum pressures remain relatively constant as a function of wave phase angle (**figure 8**). Hydrodynamic pressure distributions produce a cumulative force of **6.71 MN** for the 1-year wave and **7.25 MN** for the 50-year wave. The first of these results compares exceptionally well with the analytical result of the same value to two significant figures. The 50-year result has increased by about 5 percent.

Note on modeling: While ANSYS Aqwa enables the coupling of hydrodynamic pressures to a structural analysis module, it does not allow for the imported pressure to be ramped over a specified number of solution steps. As this is a common procedure for promoting the convergence of nonlinear computational finite element analysis solutions, it was deemed necessary to replace this load with an equivalent force distribution.

Load Summary

Table 3: Summary of aerodynamic loading.

Load	50 Year Return	1 Year Return
Operating Thrust	-	2.75 MN
Stopped Thrust, Flap	1.75 MN	-
Stopped Thrust, Edge	0.09 MN	-
Stopped Rotor Bending Moment (Mudline) Tangential to Rotor Plane, Edge	12.8 MN-m	-
Tower Drag	688 kN	54 kN

Table 4: Summary of hydrodynamic loading.

Load	50 Year Return	1 Year Return
Wave Load, Analytical	6.91 MN	6.71 MN
Wave Load, BEM (Aqwa)	7.25 MN	6.71 MN

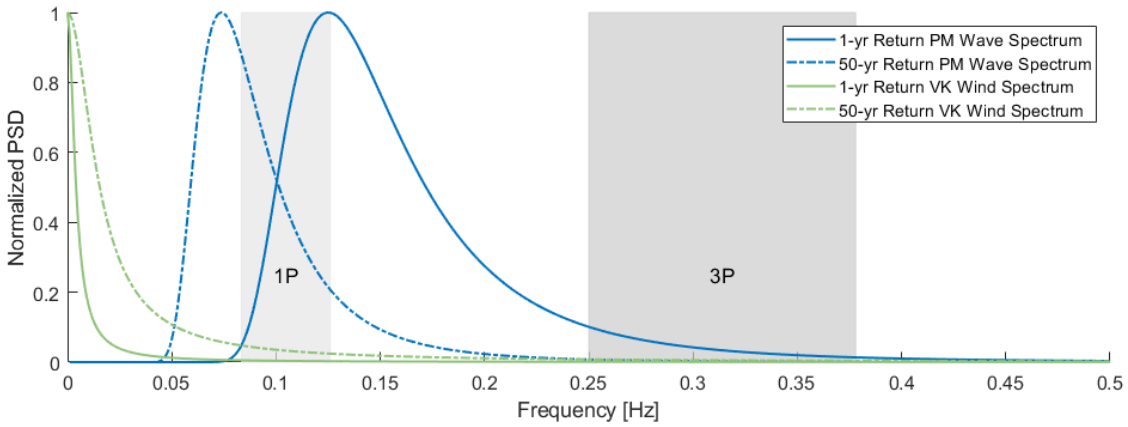

Figure 9: Normalized power spectral density for wind, wave, and passing frequency spectra.

Finite Element Model Setup

Geometry: The geometry for the IEA 15 MW was obtained from the IEA's open-source GitHub repository for the project [5]. The provided CAD model for the approximately 130 m tall tower was discretized into 10 tubular surface bodies (shells), each with a height of 13 m. Shell elements, valid for a models with a sufficiently low thickness to unsupported height ratio, offer a significant reduction in computational costs compared to a solid continuum model. When modeling thin shells (or thick shells, capable of supporting transverse shear), the surface is meshed with abstract 2D elements that are later prescribed a thickness. Here, sections are prescribed thicknesses corresponding to the tower geometry defined in **Appendix, table 12**. Sections are split down the x-z plane to enable the scoping of tower drag loads to midsection nodes (see axes in figure for reference). The geometry is shown in **figure 10**.

The IEA 10MW monopile was used as the initial starting design for the monopile. The corresponding geometry was replicated from the specifications provided in **Appendix, table 13** [4]. The 89 m monopile was discretized into 3 main sections: the non-submerged section extending 14 m above the mean water level, the 30 m submerged section, and the 45 m section embedded into the seabed. The 30 m submerged section was further divided into four sections for boundary element method modeling purposes.

The IEA 10MW monopile outer diameter is a uniform 9 m whereas the base of the IEA 15MW tower is 10 m diameter. While this may seem contradictory, This monopile was used as a first attempt for two reasons: (1) it is desirable to begin with a smaller monopile and increase dimensions if necessary (e.g. if stress limits are exceeded or natural frequencies are out of acceptable regions, etc.); and (2) the IEA 15MW, with a uniform outer diameter of 10 m, is already at the limits of modern monopile manufacturing capabilities [5]. Hence if a smaller monopile can be used, it is favorable. A simple transition piece, a solid, 1 m tall disk with a diameter of 10 m, was used in the model to transition from the 9 m monopile shell to the 10 m tower shell.

To account for the accurate weight and location of the rotor-nacelle assembly of the IEA 15MW turbine, the hub, generator, and bedplate assemblies were modeled in the geometry. The blades were not included in the analysis.

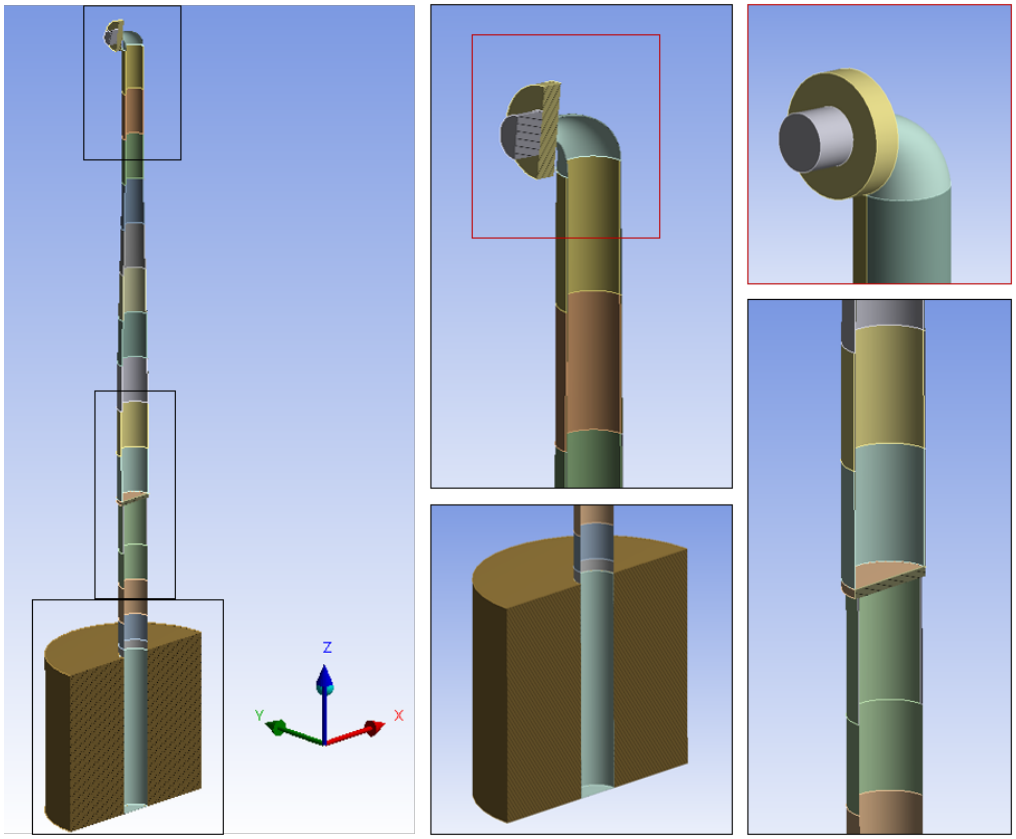

Figure 10: Model geometry.

Materials: All structural members in the model were prescribed the properties of structural steel: $\rho = 7850$ kg m^{-3}; $E = 200$ MPa; $\nu = 0.3$; $S_y = 350$ MPa; and $S_{UTS} = 460$ MPa. To account for the proper weight of the turbine rotor-nacelle assembly, the model geometries for these components were prescribed a bulk density equivalent to the specifications provided in [5]. The weight of the three blades were grouped in to the hub mass. The results of this modeling assumption are summarized in **table 5**.

Table 5: Summary of rotor, hub, generator, bedplate masses, and corresponding bulk densities used in the analysis .

	Component	Mass [t]
Bedplate Assembly	Bedplate	70
	Yaw	100
	Misc	50
Rotor Assembly	Hub	190
	Rotor	196
Generator and Shaft	Turret Nose	11.4
	In Stator	226.6
	Out Stator	145
	Shaft	15.7
	Flange	3.9
	TDO	2.2
	SRB	5.7

	Bedplate Asm	Rotor and Hub	Gen and Shaft
Total [t]:	220.3	386.1	410.5
Geom vol [m^3]:	9.0	37.7	113.5
Bulk density [kg m^{-3}]:	24589.7	10242.0	3617.1

Soil Continuum: A common approach to modeling the effects of nonlinear soil stiffness on the embedded monopile is to use the p-y model. This incorporates the use of nonlinear springs along the length and circumference of the model (depending on dimensionality). A soil continuum model was elected for use instead, however, due to the ease of use when using a commercial finite element analysis software. In literature, it is recommended that the cylindrical soil geometry have a radius of 11 times the pile diameter to simulate infinite extent of the seabed [9]. To reduce computational cost, however, the cylindrical soil continuum was reduced to a diameter of 50 m (approximately 5 times the pile diameter). To account for the nonlinearity of the soil, a standard soil material in the ANSYS geotechnical engineering materials library was used. This material incorporates the Cam-Clay soil model, an elastic plastic strain hardening model. The material also employs a a porous elasticity model with a swell index of 0.0024, elastic tensile strength limit of 34.5 kPa, a Poisson's ratio of 0.279, and an initial void ratio of 0.3.

A complete summary of of material properties is shown in **table 6**.

Table 6: Materials used in the finite element model.

Structural Steel

Property	Value	Unit
Material Field Variables	Table	
Density	7850	kg m^-3
Isotropic Secant Coefficient of Thermal Expansion		
Isotropic Elasticity		
Derive from	Young's ...	
Young's Modulus	2E+11	Pa
Poisson's Ratio	0.3	
Bulk Modulus	1.6667E+11	Pa
Shear Modulus	7.6923E+10	Pa
Strain-Life Parameters		
S-N Curve	Tabular	
Tensile Yield Strength	2.5E+08	Pa
Compressive Yield Strength	2.5E+08	Pa
Tensile Ultimate Strength	4.6E+08	Pa
Compressive Ultimate Strength	0	Pa

Soil Model

Property	Value	Unit
Material Field Variables	Table	
Density	1	kg m^-3
Cam-Clay		
Plastic Slope Parameter	0.014	
Slope of Critical State Line	1.24	
Initial Size of Yield Surface	2.4132E+05	Pa
Minimum Size of Yield Surface	2413.2	Pa
Dry Part of Yield Surface Modifier	1	
Wetting Part of Yield Surface Modifier	1	
Anisotropic Yield Surface Parameter	1	
Porous Elasticity		
Swell Index	0.0024	
Elastic Limit of Tensile Strength	34474	Pa
Poisson's Ratio	0.279	
Initial Void Ratio	0.3	

Contacts: All contacting surface bodies and solid models are prescribed a bonded connection type. Bonded connections do not allow for sliding between surfaces and prohibits the formation of gaps between bonded edges and faces. Tower and monopile shell sections are bonded to one another at the edges, as to simulate a welded interface. While the interface between the embedded monopile and the soil continuum should likely be modeled with a friction-based contact type for the most realistic results, a bonded interface was elected to avoid the introduction of more nonlinearities into the analysis.

Mesh: A total of 16,686 structural elements were used to mesh the tower and monopile structures. The maximum allowable mesh size on these structures was set to 0.75 m. A majority of the elements were 2D shell elements, owing to the relatively low element count. An additional 30,000 elements were devoted to the soil continuum model, meshed with a multi-zone, hex-dominant method. A division-based edge sizing was scoped to the circumference of the cylindrical soil geometry to ensure a uniform mesh. The meshed geometry is shown in **figure 11**

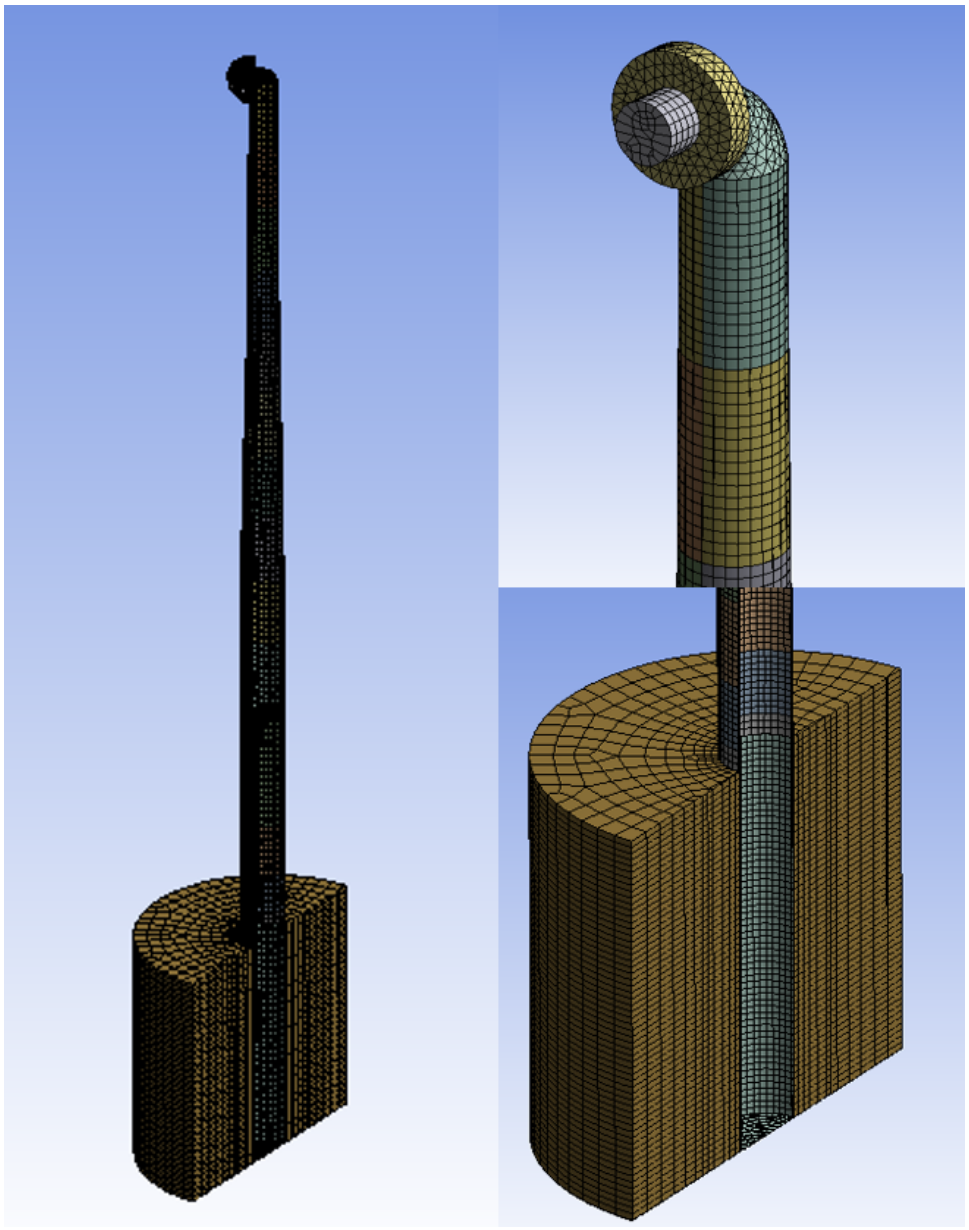

Figure 11: Mesh.

Analysis Subsystems

Workflow: The ANSYS Workbench project is composed of four main analysis subsystems: (1) a hydrodynamic diffraction analysis (discussed in **Hydrodynamic Load Calculations**); (2) a nonlinear static structural analysis; (3) a modal analysis; and (4) an eigenvalue buckling analysis. A common geometry is shared between all subsystems. Tower drag forces for the 1-year and 50-year winds, externally calculated in the MATLAB script, are fed into the nonlinear static structural analysis. An additional linear static structural analysis subsystem is also needed for the buckling analysis, which will be explained later in this section. All subsystems are routed to a central parameter set, which enables the parametric optimization of the monopile diameter, wall thickness, and embedment length, as well as the diameter of the soil continuum radius. The project workflow is shown in **Figure 12**

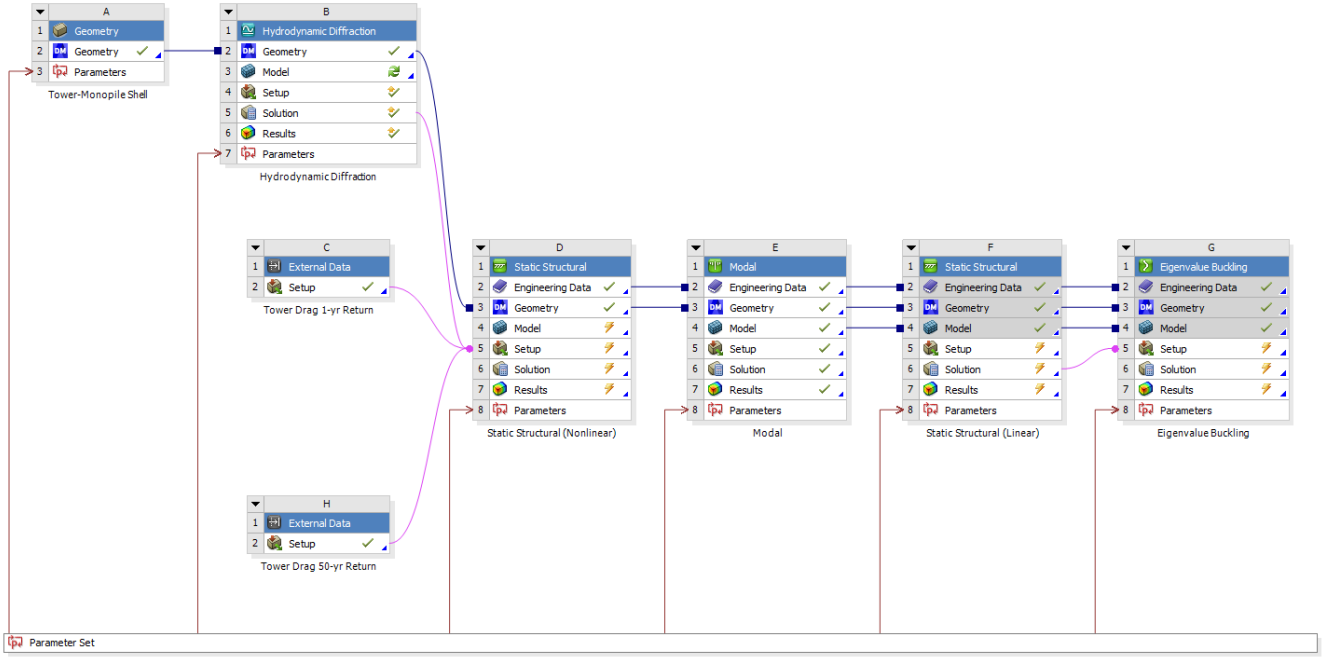

Figure 12: ANSYS project workflow.

Nonlinear Static Structural Analysis: The nonlinear structural analysis is the primary simulation used to obtain estimates of stresses and deflection. It incorporates the all of the aerodynamic, hydrodynamic, and gravitational loads, and models the soil continuum (the source of nonlinearity). To promote convergence, all applied loads were ramped over four time steps.

Modal Analysis: The ANSYS modal analysis module does not permit the use of nonlinear materials and/or nonlinear boundary conditions. Consequently, it was not possible to include the soil continuum model in the analysis. As a replacement, elastic support boundary conditions were scoped to the embedded surfaces of the monopile. An average secant elastic modulus of 80 MPa (dense sand, drained) was used for the stiffness of the support (Budhu, M. *Soil Mechanics and Foundations*). The modal analysis subsystem is set to calculate the first 6 modes.

Eigenvalue Buckling Analysis: An eigenvalue buckling analysis (linear) was prepared with the same linear soil boundary conditions as the modal analysis subsystem. The simulation reports a load multiplier that corresponds to a ratio of the calculated buckling load to the applied load. In this simulation, the only applied loads are the gravitational loads: the weight of the RNA, tower, and monopile. This subsystem requires a static structural analysis to be present, hence the need for a linear static structural subsystem adjacent to the eigenvalue buckling subsystem in the project workflow.

Initial Results

Two simulations were run for the initial design borrowed from the IEA 10MW: a 1-year return case and a 50-year return case. Both models applied the loads summarized in **Load Summary, 3 and 4**. As the flapwise loads for the 50-year return load case are shown to be much more severe than the 1-year loads, the 1-year loads are not simulated. Loads are applied in the worst case scenario: operating thrust (or stopped rotor drag), tower drag, and wave loading are all applied in the same direction. Results for fundamental frequency, critical buckling load, maximum stress, and maximum deflection for the two simulations are presented in **table 7**. Regions of maximum stress are shown in **figure 13**. Similarly, the 1-year load case deflection and the first modal shape are depicted in **figure 14**. Results for both the 1-year and 50-year return load cases meet the metrics of the design based on the allowable limits provided by the developer in **Introduction, table 2** and the specified material properties. A 0.17 Hz frequency limit was imposed based on the normalized power spectral density plot shown in **Load Summary, figure 9**. The results indicate the initial monopile design borrowed from the IEA 10 MW is satisfactory.

Table 7: Summary of initial results for IEA 10MW monopile simulation.

Result	50 Year Return	1 Year Return	Allowable
Fundamental Frequency	0.1754 Hz	0.1754 Hz	>0.17 Hz
Critical Buckling Load Multiplier	3.96	3.96	>2
Maximum Equivalent Stress	265.1 MPa	181.8 MPa	<350 MPa
Maximum Deflection	1.29 m	0.65 m	<1.5 m

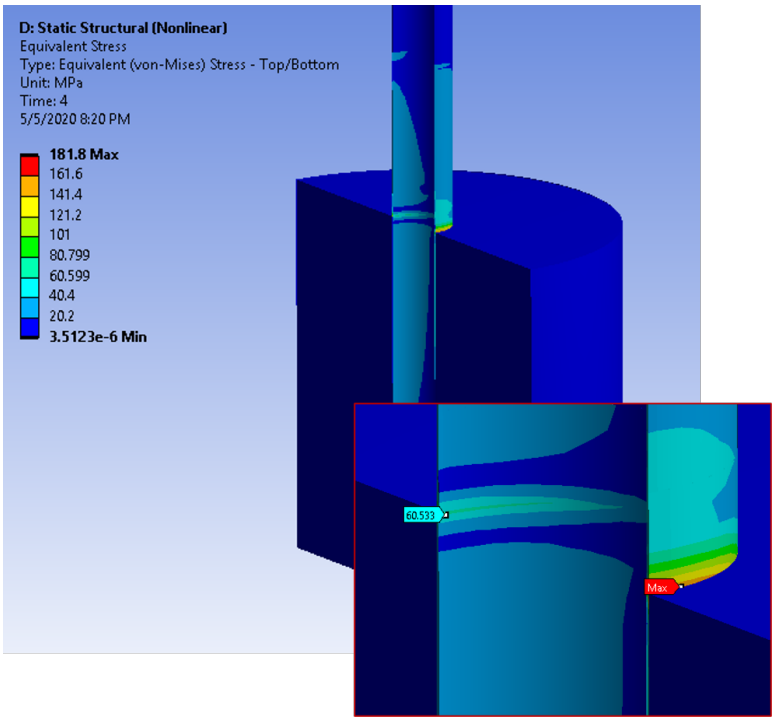

Figure 13: Stress for the 1-yr return case.

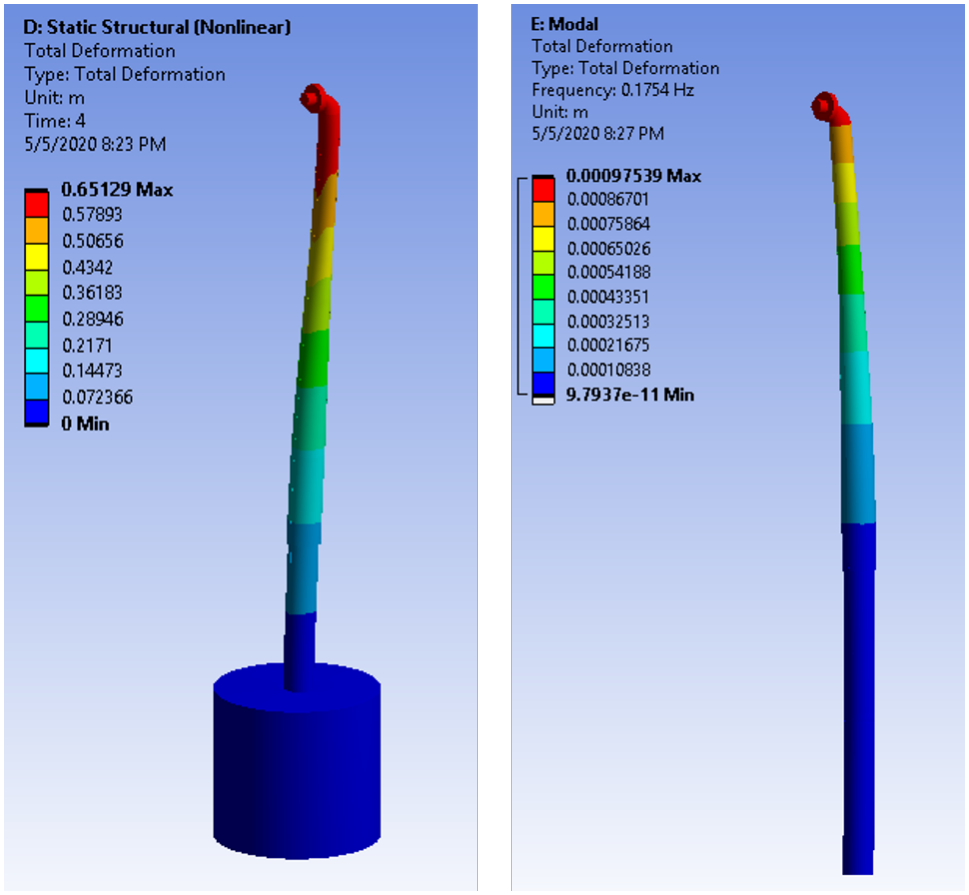

Figure 14: (Left) Deflection for the 1-yr return case; (Right) First modal shape (side-side).

Parametric Optimization

Initial results proved the IEA 10MW monopile design to be satisfactory. This design, however, has average wall thickness of 100 mm. Consequently, the mass of the 90 m monopile structure (with an embedment length of 45 m) totals to just under 1000 tons. In an effort to seek a design that achieves comparable performance at a lower mass, a parametric optimization was performed with in ANSYS Workbench. In the set-up of the optimization, monopile thickness and fundamental frequency were parameterized and fundamental frequency was selected as the optimization target. Fundamental frequency was identified as the optimization target for the following reasons: (1) the fundamental frequency is shown to be highly sensitive to the structure diameter and thickness; (2) the fundamental frequency has a strict, narrow range of allowable values and is already close to its acceptable limit of 0.17 Hz in the initial design; and (3) the modal analysis subsystem is linear and thus capable of running many iterations relatively quickly. The 0.17 Hz limit is depicted on the PSD plot in **figure 15**.

Design Points: Only two monopile diameters were considered: 9 m and 10 m. Thickness was allowed to vary from 50 to 100 mm in increments of 5 mm. As the maximum deflection for the initial design is close the 1% limit of 1.5 m, the monopile embedment length of 45 m was left unaltered for all design points. The workflow for the parametric optimization is shown in **figure 16**

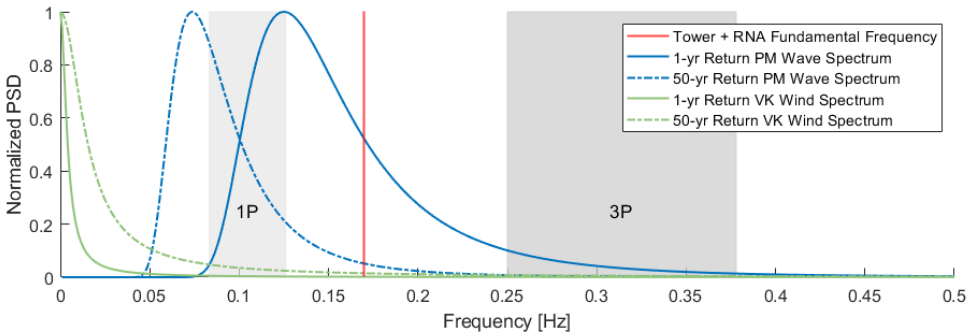

Figure 15: Minimum acceptable fundamental frequency of $f_n = 0.17$ Hz.

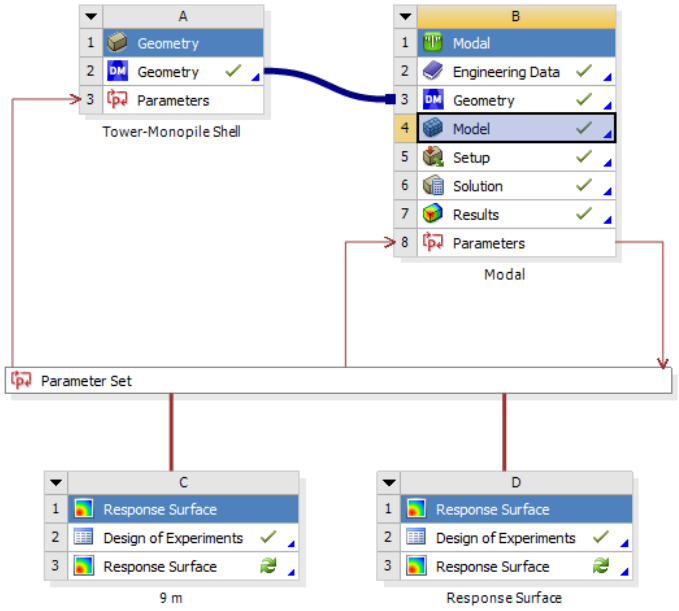

Figure 16: Optimization Workflow.

Results: Parametric optimization results are shown in **figure 17**. Fundamental frequency is shown to exhibit a weak logarithmic behavior with increasing monopile thickness. Using the minimum allowable fundamental frequency of 1.7 Hz, the optimization results were interpolated to identify the corresponding thickness for both the 9 and 10 m diameter monopiles. To meet the minimum frequency requirement, a 9 m diameter monopile requires a minimum thickness of approximately 87.5 mm while a 10 m monopile only requires a thickness of 64 mm. These values correspond to masses of 700 and 875 kg, respectively; the 10 m monopile is able to meet the same frequency limits using much less material. The 90 m long monopile (45 m of embedment) with a diameter of 10 m and a uniform wall thickness of 65 mm was chosen as the subject for the the final round of simulations.

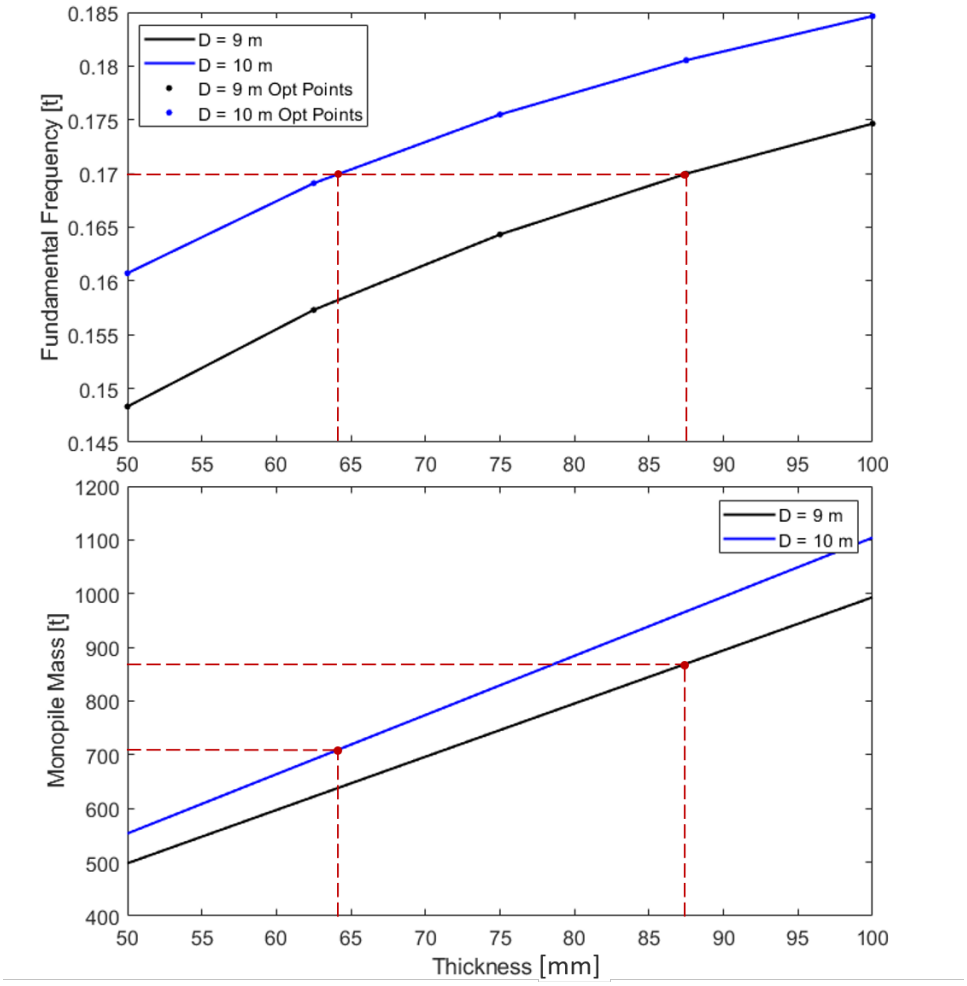

Figure 17: (Top) Optimization results: fundamental frequency as a function of monopile thickness. The allowable fundamental frequency limit is traced to both curves and the and corresponding monopile thickness is identified (red dashed line for both curves); (Bottom) Monopile mass as a function of thickness. Corresponding thicknesses from the optimization results are used to identify the monopile mass for both curves (red dashed line).

Final Results and Recommendation

Summary of Results: Two final simulations were run for the monopile optimized for the fundamental frequency limit of 1.7 Hz: a 90 m long monopile (45 m of embedment) with a diameter of 10 m and a uniform wall thickness of 65 mm. All loads and boundary conditions used in the final simulation were exactly the same as in the initial simulation. The results are shown in **table 8**. The fundamental frequency, maximum equivalent stress, and maximum deflection for the 50-year return period are incredibly close to their respective limits. The monopile is near optimal, but the wall thickness should be increased to guarantee reliability during 50-year conditions, despite the unlikeness of such events during a turbine's 20-yr design life.

Final Recommendation: Two monopiles have been shown to be satisfactory for the IEA 15MW turbine operating in the proposed conditions. The 90 m IEA 15 MW monopile with a diameter of 9 m is the more conservative of the options, though it uses approximately 1000 t of material. The 10 m diameter monopile of similar length with a uniform wall thickness of 65 mm meets the requirements with a margin of safety for the 50-year return condition, however it uses only 700 t of material. The safety of this monopile can be improved by increasing the thickness to 70 mm or greater while still maintaining a lower weight than the IEA 10 MW monopile.

Table 8: Summary of final results for the 10 m diameter monopile simulation.

Result	50 Year Return	1 Year Return	Allowable
Fundamental Frequency	0.17 Hz	0.17 Hz	>0.17 Hz
Critical Buckling Load Multiplier	3.78	3.78	>2
Maximum Equivalent Stress	330.24 MPa	250.51 MPa	<350 MPa
Maximum Deflection	1.42 m	0.95 m	<1.5 m

Table 9: Summary of initial results for IEA 10MW monopile simulation.

Result	50 Year Return	1 Year Return	Allowable
Fundamental Frequency	0.1754 Hz	0.1754 Hz	>0.17 Hz
Critical Buckling Load Multiplier	3.96	3.96	>2
Maximum Equivalent Stress	265.1 MPa	181.8 MPa	<350 MPa
Maximum Deflection	1.29 m	0.65 m	<1.5 m

Appendix

Turbine Specifications: IEA 15 MW

Table 10: IEA 15 MW Offshore Wind Turbine Specifications [5].

Table ES-1. Key Parameters for the IEA Wind 15-MW Turbine

Parameter	Units	Value
Power rating	MW	15
Turbine class	-	IEC Class 1B
Specific rating	W/m^2	332
Rotor orientation	-	Upwind
Number of blades	-	3
Control	-	Variable speed Collective pitch
Cut-in wind speed	m/s	3
Rated wind speed	m/s	10.59
Cut-out wind speed	m/s	25
Design tip-speed ratio	-	9 0
Minimum rotor speed	rpm	5.0
Maximum rotor speed	rpm	7.56
Maximum tip speed	m/s	95
Rotor diameter	m	240
Airfoil series	-	FFA-W3
Hub height	m	150
Hub diameter	m	7.94
Hub overhang	m	11.35
Rotor precone angle	deg	-4.0
Blade prebend	m	4
Blade mass	t	65
Drivetrain	-	Direct drive
Shaft tilt angle	deg	6
Rotor nacelle assembly mass	t	1,017
Transition piece height	m	15
Monopile embedment depth	m	45
Monopile base diameter	m	10
Tower mass	t	860
Monopile mass	t	1,318

deg	degrees	rpm	revolutions per minute
m	meters	t	metric tons
m/s	meters per second	W/m^2	watts per square meter

Table 11: IEA 15 MW Blade Properties [5].

Table ES-2. Blade Properties

Description	Value	Units
Blade length	117	m
Root diameter	5.20	m
Root cylinder length	2.34	m
Max chord	5.77	m
Max chord spanwise position	27.2	m
Tip prebend	4.00	m
Precone	4.00	deg
Blade mass	65,250	kg
Blade center of mass	26.8	m
Design tip-speed ratio	9.00	-
First flapwise natural frequency	0.555	Hz
First edgewise natural frequency	0.642	Hz
Design C_P	0.489	-
Design C_T	0.799	-
Annual energy production	77.4	GWh

deg	degrees	kg	kilograms
GWh	gigawatt-hours	m	meters
Hz	Hertz		

Tower Specifications: IEA 15 MW

Table 12: IEA 15 MW Tower Geometry [5].

Location	Height [m]	Outer Diameter [m]	Thickness [mm]
Monopile start	-75.000	10.000	55.341
Mud line	-30.000	10.000	55.341
	-29.999	10.000	55.341
	-25.000	10.000	55.341
	-24.999	10.000	53.449
	-20.000	10.000	53.449
	-19.999	10.000	51.509
	-15.000	10.000	51.509
	-14.999	10.000	49.527
	-10.000	10.000	49.527
	-9.999	10.000	47.517
	-5.000	10.000	47.517
	-4.999	10.000	45.517
Water line	0.000	10.000	45.517
	0.001	10.000	43.527
	5.000	10.000	43.527
	5.001	10.000	42.242
	10.000	10.000	42.242
	10.001	10.000	41.058
Tower start	15.000	10.000	41.058
	15.001	10.000	39.496
	28.000	10.000	39.496
	28.001	10.000	36.456
	41.000	9.926	36.456
	41.001	9.926	33.779
	54.000	9.443	33.779
	54.001	9.443	32.192
	67.000	8.833	32.192
	67.001	8.833	30.708
	80.000	8.151	30.708
	80.001	8.151	29.101
	93.000	7.390	29.101
	93.001	7.390	27.213
	106.000	6.909	27.213
	106.001	6.909	24.009
	119.000	6.748	24.009
	119.001	6.748	20.826
	132.000	6.572	20.826
	132.001	6.572	23.998
Tower top	144.582	6.500	23.998

Starting Design Reference: IEA 10 MW Monopile

Table 13: IEA 10 MW Monopile Geometry [4].

Location [-]	z [m]	D_o [m]	D_i [m]	$I_{xx} = I_{yy}$ [m^4]	J [m^4]
Yaw bearing	145.63	5.5	5.44	2.03	4.07
	134.55	5.79	5.73	2.76	5.52
	124.04	6.07	6.00	3.63	7.26
	113.54	6.35	6.26	4.67	9.35
	103.03	6.63	6.53	5.90	11.80
	92.53	6.91	6.80	7.33	14.67
	82.02	7.19	7.07	8.99	17.98
	71.52	7.46	7.34	10.9	21.80
	61.01	7.74	7.61	13.08	26.15
↑	50.51	8.02	7.88	15.55	31.09
tower	40.00	8.30	8.16	15.55	31.09
foundation	40.00	9.00	8.70	34.84	69.68
↓	38.00	9.00	8.70	35.74	71.48
	36.00	9.00	8.70	36.66	73.32
	34.00	9.00	8.70	37.59	75.18
	32.00	9.00	8.69	38.54	77.08
waterline	30.00	9.00	8.69	39.51	79.01
	28.00	9.00	8.69	40.49	80.97
	26.00	9.00	8.69	41.48	82.97
	24.00	9.00	8.69	42.50	85.00
	22.00	9.00	8.69	43.53	87.05
	20.00	9.00	8.69	44.05	88.10
	16.00	9.00	8.80	28.09	56.18
	12.00	9.00	8.80	28.09	56.18
	8.00	9.00	8.80	28.09	56.18
	4.00	9.00	8.80	28.09	56.18
mudline	0.00	9.00	8.80	28.09	56.18
	-8.40	9.00	8.80	28.09	56.18
	-16.80	9.00	8.80	28.09	56.18
	-25.20	9.00	8.80	28.09	56.18
	-33.60	9.00	8.80	28.09	56.18
	-42.60	9.00	8.80	28.09	56.18

Stopped Turbine Thrust Force Results

Table 14: Blade forces for $\theta_{p,0} = 90$ deg (feathered). The sum of differential normal forces yields a thrust of 87.3 kN.

Distance [m]	CL	CD	Twist [deg]	Alpha [deg]	Phi [deg]	dF_D [N]	dF_L [N]	dFt [N]	dFn [N]
1.17	0.000	0.3500	15.59	-15.59	90.00	4177	1	4	12531
3.51	-0.047	0.3425	15.51	-15.51	90.00	4101	-565	-1695	12303
5.85	-0.205	0.3160	15.21	-15.21	90.00	3813	-2477	-7432	11439
8.19	-0.439	0.2720	14.65	-14.65	90.00	3322	-5365	-16095	9965
10.53	-0.654	0.2204	13.90	-13.90	90.00	2731	-8101	-24304	8193
13.16	-0.782	0.1655	12.89	-12.89	90.00	2609	-12327	-36981	7826
16.09	-0.801	0.1165	11.66	-11.66	90.00	1871	-12866	-38597	5612
18.66	-0.741	0.0858	10.55	-10.55	90.00	1064	-9193	-27578	3191
20.89	-0.687	0.0651	9.63	-9.63	90.00	815	-8592	-25777	2444
23.12	-0.635	0.0470	8.81	-8.81	90.00	591	-7987	-23962	1772
25.34	-0.598	0.0335	8.10	-8.10	90.00	421	-7522	-22567	1263
27.57	-0.552	0.0259	7.48	-7.48	90.00	324	-6902	-20707	973
29.91	-0.500	0.0219	6.85	-6.85	90.00	296	-6780	-20341	889
32.36	-0.435	0.0188	6.21	-6.21	90.00	249	-5774	-17323	747
34.80	-0.369	0.0169	5.59	-5.59	90.00	218	-4765	-14294	654
37.25	-0.297	0.0153	5.01	-5.01	90.00	192	-3723	-11168	576
39.77	-0.237	0.0139	4.47	-4.47	90.00	179	-3039	-9118	536
42.35	-0.176	0.0126	3.96	-3.96	90.00	157	-2192	-6576	471
44.93	-0.110	0.0120	3.52	-3.52	90.00	145	-1335	-4004	436
47.51	-0.058	0.0114	3.11	-3.11	90.00	135	-690	-2071	405
50.09	-0.006	0.0109	2.74	-2.74	90.00	125	-68	-205	375
52.54	0.036	0.0103	2.41	-2.41	90.00	103	356	1069	309
54.84	0.081	0.0096	2.12	-2.12	90.00	94	794	2381	282
57.15	0.129	0.0090	1.85	-1.85	90.00	86	1231	3693	258
59.45	0.163	0.0085	1.59	-1.59	90.00	79	1511	4533	236
61.76	0.206	0.0081	1.34	-1.34	90.00	73	1867	5600	220
64.08	0.233	0.0078	1.10	-1.10	90.00	70	2099	6297	210
66.44	0.256	0.0075	0.88	-0.88	90.00	66	2259	6776	198
68.79	0.279	0.0073	0.68	-0.68	90.00	62	2399	7196	187
71.14	0.302	0.0071	0.48	-0.48	90.00	60	2531	7592	179
73.49	0.326	0.0071	0.28	-0.28	90.00	58	2662	7985	173
75.79	0.351	0.0071	0.09	-0.09	90.00	54	2653	7960	161
78.02	0.378	0.0072	-0.10	0.10	90.00	53	2785	8355	159
80.25	0.406	0.0073	-0.31	0.31	90.00	52	2914	8743	156
82.48	0.446	0.0073	-0.55	0.55	90.00	51	3123	9370	154
84.71	0.475	0.0074	-0.83	0.83	90.00	50	3232	9696	151
86.95	0.514	0.0075	-1.13	1.13	90.00	49	3403	10210	148
89.18	0.551	0.0076	-1.43	1.43	90.00	49	3547	10640	146
91.95	0.599	0.0077	-1.76	1.76	90.00	71	5499	16496	212
94.70	0.623	0.0078	-2.02	2.02	90.00	45	3647	10940	136
96.89	0.634	0.0078	-2.14	2.14	90.00	44	3592	10776	132
99.08	0.646	0.0078	-2.17	2.17	90.00	43	3529	10588	128
101.28	0.646	0.0078	-2.17	2.17	90.00	41	3397	10190	123
103.47	0.634	0.0078	-2.14	2.14	90.00	39	3202	9607	118
105.67	0.634	0.0078	-2.08	2.08	90.00	38	3066	9198	113
107.86	0.623	0.0078	-2.00	2.00	90.00	36	2873	8620	108
110.05	0.611	0.0077	-1.88	1.88	90.00	34	2682	8046	102
112.61	0.587	0.0077	-1.69	1.69	90.00	42	3230	9690	127
115.54	0.552	0.0076	-1.41	1.41	90.00	25	1857	5571	76

Table 15: Blade forces for $\theta_{p,0} = 0$ deg (flapwise). The sum of differential normal forces yields a thrust of 1.74 MN.

Distance [m]	CL	CD	Twist [deg]	Alpha [deg]	Phi [deg]	dF_D [N]	dF_L [N]	dFt [N]	dFn [N]
1.17	0.000	0.3500	15.59	74.41	90.00	4177	1	4	12531
3.51	0.013	0.3842	15.51	74.49	90.00	4601	156	467	13803
5.85	0.056	0.5021	15.21	74.79	90.00	6060	677	2030	18179
8.19	0.120	0.6887	14.65	75.35	90.00	8409	1463	4388	25228
10.53	0.178	0.8869	13.90	76.10	90.00	10986	2207	6621	32959
13.16	0.220	1.0620	12.89	77.11	90.00	16735	3473	10419	50205
16.09	0.237	1.1761	11.66	78.34	90.00	18882	3802	11406	56645
18.66	0.230	1.2230	10.55	79.45	90.00	15162	2848	8543	45487
20.89	0.220	1.2451	9.63	80.37	90.00	15574	2749	8247	46722
23.12	0.209	1.2616	8.81	81.19	90.00	15858	2628	7884	47574
25.34	0.197	1.2720	8.10	81.90	90.00	15992	2480	7440	47977
27.57	0.185	1.2768	7.48	82.52	90.00	15963	2316	6949	47890
29.91	0.172	1.2801	6.85	83.15	90.00	17352	2329	6988	52056
32.36	0.156	1.2835	6.21	83.79	90.00	17029	2067	6201	51088
34.80	0.142	1.2864	5.59	84.41	90.00	16619	1835	5506	49857
37.25	0.128	1.2894	5.01	84.99	90.00	16171	1611	4834	48514
39.77	0.117	1.2919	4.47	85.53	90.00	16572	1500	4500	49717
42.35	0.105	1.2939	3.96	86.04	90.00	16109	1307	3920	48327
44.93	0.093	1.2946	3.52	86.48	90.00	15687	1127	3380	47060
47.51	0.083	1.2952	3.11	86.89	90.00	15292	982	2947	45877
50.09	0.074	1.2958	2.74	87.26	90.00	14897	849	2546	44690
52.54	0.067	1.2995	2.41	87.59	90.00	12997	672	2017	38990
54.84	0.061	1.3122	2.12	87.88	90.00	12805	596	1789	38415
57.15	0.055	1.3343	1.85	88.15	90.00	12703	524	1572	38110
59.45	0.051	1.3609	1.59	88.41	90.00	12640	474	1423	37921
61.76	0.045	1.3865	1.34	88.66	90.00	12566	405	1214	37698
64.08	0.040	1.4103	1.10	88.90	90.00	12730	361	1084	38189
66.44	0.035	1.4358	0.88	89.12	90.00	12645	305	916	37934
68.79	0.029	1.4617	0.68	89.32	90.00	12560	247	741	37681
71.14	0.023	1.4828	0.48	89.52	90.00	12430	190	569	37290
73.49	0.017	1.4950	0.28	89.72	90.00	12221	137	411	36663
75.79	0.011	1.4990	0.09	89.91	90.00	11338	85	256	34013
78.02	0.006	1.4995	-0.10	90.10	90.00	11060	45	136	33180
80.25	0.001	1.4996	-0.31	90.31	90.00	10776	10	30	32327
82.48	-0.005	1.4992	-0.55	90.55	90.00	10488	-38	-113	31465
84.71	-0.010	1.4990	-0.83	90.83	90.00	10205	-66	-198	30614
86.95	-0.016	1.4984	-1.13	91.13	90.00	9920	-106	-317	29760
89.18	-0.022	1.4977	-1.43	91.43	90.00	9635	-142	-427	28904
91.95	-0.030	1.4968	-1.76	91.76	90.00	13739	-280	-839	41217
94.70	-0.035	1.4964	-2.02	92.02	90.00	8763	-203	-609	26288
96.89	-0.037	1.4961	-2.14	92.14	90.00	8472	-208	-624	25416
99.08	-0.039	1.4959	-2.17	92.17	90.00	8172	-212	-637	24516
101.28	-0.039	1.4959	-2.17	92.17	90.00	7865	-204	-613	23595
103.47	-0.037	1.4961	-2.14	92.14	90.00	7552	-185	-556	22657
105.67	-0.037	1.4961	-2.08	92.08	90.00	7231	-178	-533	21693
107.86	-0.035	1.4964	-2.00	92.00	90.00	6904	-160	-480	20713
110.05	-0.033	1.4966	-1.88	91.88	90.00	6570	-143	-429	19711
112.61	-0.028	1.4970	-1.69	91.69	90.00	8235	-156	-468	24704
115.54	-0.022	1.4977	-1.41	91.41	90.00	5041	-74	-223	15123

Tower Loads

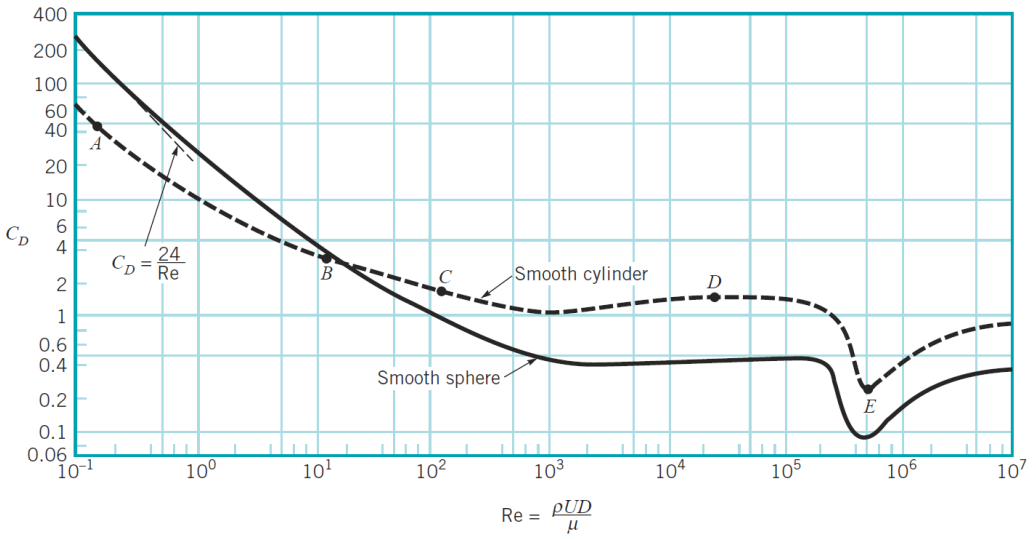

Figure 18: Drag coefficient data for a smooth cylinder used in the tower aerodynamic loading calculation. Obtained from Munson et al. *Fundamentals of Fluid Mechanics, 6e.*

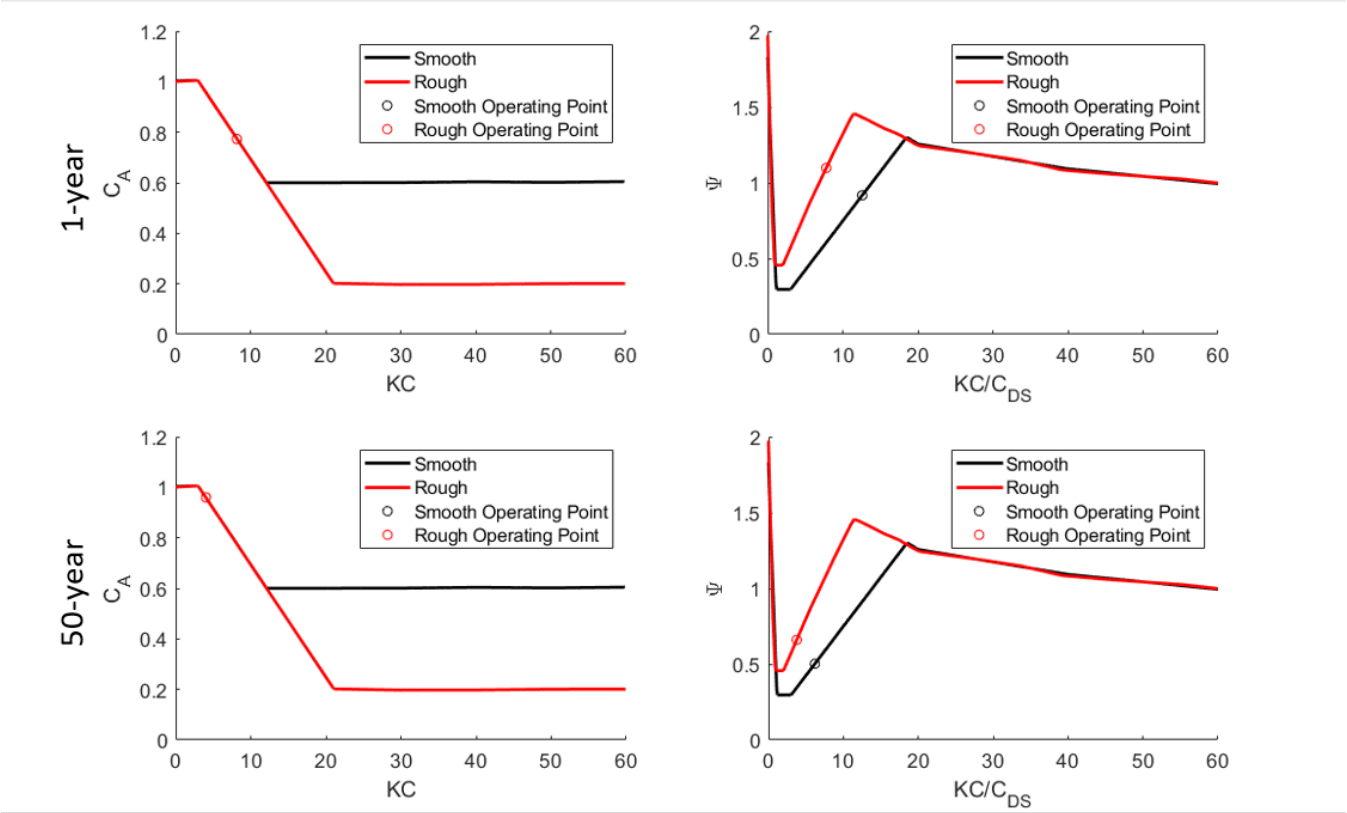

Figure 19: Morison drag and added mass coefficient operating points for 1-year wave (top) and 50-year wave (bottom). Cds Rough = 1.05 and Cds Smooth = 0.65. [7]

References

[1] "IEC 61400-1: Wind energy generation systems – part 1: Design requirements," International Electrotechnical Commision, Tech. Rep., 2014.

[2] "IEC 61400-3-1: : Wind energy generation systems – part 3-1: Design requirements for fixed offshore wind turbines," International Electrotechnical Commision, Tech. Rep., 2018.

[3] J. Manwell and K. Sharman, "Specifications for a monopile offshore wind energy generation platform," University of Massachusetts Amherst, Department of Mechanical and Industrial Engineering, Tech. Rep., 2020.

[4] P. Bortolotti, H. C. Tarres, K. Dykes, K. Merz, L. Sethuraman, D. Verelst, and F. Zahle, "Iea wind task 37 on systems engineering in wind energy – wp2.1 reference wind turbines," NREL/TP-73492, International Energy Agency, Tech. Rep., 2019. [Online]. Available: https://www.nrel.gov/docs/fy19osti/73492.pdf

[5] E. Gaertner, J. Rinker, L. Sethuraman, F. Zahle, B. Anderson, G. Barter, N. Abbas, F. Meng, P. Bortolotti, W. Skrzypiński, G. Scott, R. Feil, H. Bredmose, K. Dykes, M. Shields, C. Allen, A. Viselli, N. R. E. Laboratory, and G. Co, "Definition of the international energy agency 15-megawatt offshore reference wind turbine," NREL/TP-5000-75698, National Renewable Energy Laboratory, Golden, CO, Tech. Rep., 2020.

[6] B. Pereyra, F. Wendt, A. Robertson, and J. Jonkman, "Assessment of first- and second-order wave-excitation load models for cylindrical substructures: Preprint," p. 7.

[7] G. DNV, "DNV-OS-j101: Design of offshore wind turbine structures," p. 238.

[8] O. B. Leite, "Review of design procedures for monopile offshore wind structures," p. 146.

[9] N. Strömblad, "Modeling of soil and structure interaction subsea," p. 70.